

*ATS drugs molecular structure  
representation using refined 3D geometric  
moment invariants*

**Satrya Fajri Pratama, Azah Kamilah  
Muda, Yun-Huoy Choo, Jan Flusser &  
Ajith Abraham**

**Journal of Mathematical Chemistry**

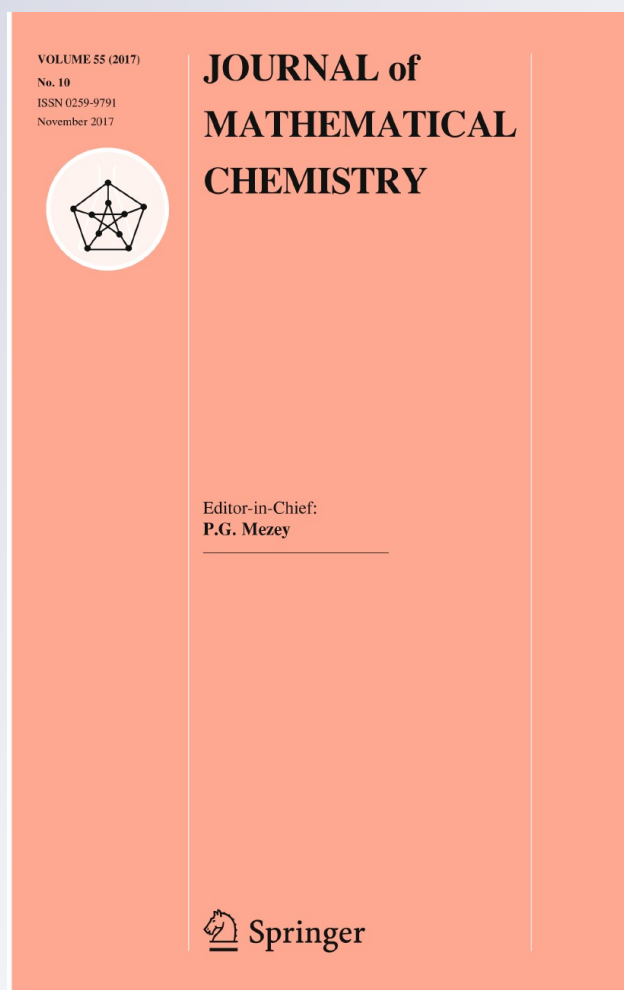
ISSN 0259-9791

Volume 55

Number 10

J Math Chem (2017) 55:1951-1963

DOI 10.1007/s10910-017-0775-3



**Your article is protected by copyright and all rights are held exclusively by Springer International Publishing AG. This e-offprint is for personal use only and shall not be self-archived in electronic repositories. If you wish to self-archive your article, please use the accepted manuscript version for posting on your own website. You may further deposit the accepted manuscript version in any repository, provided it is only made publicly available 12 months after official publication or later and provided acknowledgement is given to the original source of publication and a link is inserted to the published article on Springer's website. The link must be accompanied by the following text: "The final publication is available at [link.springer.com](http://link.springer.com)".**

# ATS drugs molecular structure representation using refined 3D geometric moment invariants

Satrya Fajri Pratama<sup>1</sup> · Azah Kamilah Muda<sup>1</sup> · Yun-Huoy Choo<sup>1</sup> · Jan Flusser<sup>2</sup> · Ajith Abraham<sup>1,3</sup>

Received: 24 June 2016 / Accepted: 22 June 2017 / Published online: 28 June 2017  
© Springer International Publishing AG 2017

**Abstract** The campaign against drug abuse is fought by all countries, most notably on ATS drugs. The identification process of ATS drugs depends heavily on its molecular structure. However, the process becomes more unreliable due to the introduction of new, sophisticated, and increasingly complex ATS molecular structures. Therefore, distinctive features of ATS drug molecular structure need to be accurately obtained. In this paper, two variants of refined 3D geometric moment invariants for ATS drug molecular structure representation are discussed. This paper is also meant for comparing the performance of these two variants. The comparison was conducted using drug chemical structures obtained from Isomer Design's PiHKaL.info database for the ATS drugs, while non-ATS drugs are obtained randomly from ChemSpider database. The

---

✉ Azah Kamilah Muda  
azah@utem.edu.my

Satrya Fajri Pratama  
satrya@student.utem.edu.my

Yun-Huoy Choo  
huoy@utem.edu.my

Jan Flusser  
flusser@utia.cas.cz

Ajith Abraham  
ajith.abraham@ieee.org

- <sup>1</sup> Computational Intelligence and Technologies (CIT) Research Group, Center of Advanced Computing and Technologies, Faculty of Information and Communication Technology, Universiti Teknikal Malaysia Melaka, Hang Tuah Jaya, 76100 Durian Tunggal, Melaka, Malaysia
- <sup>2</sup> Institute of Information Theory and Automation of ASCR, Pod Vodárenskou věží 4, 182 08 Prague 8, Czech Republic
- <sup>3</sup> Machine Intelligence Research Labs (MIR Labs), Scientific Network for Innovation and Research Excellence, Auburn, WA, USA

assessment highlights the best technique which is suitable to be further explored and improved in the future studies so that it is wholly attuned with ATS drug molecular similarity search domain.

**Keywords** 3D moment invariants · Geometric moment invariants · ATS drugs · Molecular similarity · Molecular descriptors

## 1 Introduction

Amphetamine-type Stimulants (ATS) drug abuse, such as amphetamine, methamphetamine, and substances of the “ecstasy”-group, is recognized as universal, disturbing social delinquents. The struggles of finding tangible resolution of drugs abuse prevention are encountered by every national law enforcement authorities, because of the presence of new variety or unidentified ATS drugs. Nevertheless, the focus of cheminformatics research community is toward the advancement of chemical compounds that induces preferred biological outcome. Contrariwise, less devotion is demonstrated to the molecular similarity search which can be used to identify unfamiliar substances.

Ordinarily, the identification process depends on the chemical composition and conformation of a molecule, or generally referred as molecular structure. However, relying on these criteria alone for identification has been proved to be more undependable, mainly because the designs of novel ATS molecular structures are continuously more complex and sophisticated. Furthermore, it is a challenge for national law enforcement authorities and scientific staff of forensic laboratories, because present testing unit is very inadequate to identify new variety or unidentified ATS drug, in addition to likely detecting false negatives.

Geometrical shapes have been used for a long time to represent two-dimensional (2D) and three-dimensional (3D) molecular structures, and these geometric shapes can be described numerically using shape descriptors. There are two types of 2D shape descriptors, which are boundary-based and area-based. On the other hand, 3D shape descriptors are emphasized into volume- and surface-based descriptors. It is commonly pronounced that 3D shape descriptor as more potent and more correctly represents an object's shape. Thus, this study believes that 3D descriptor is capable to identify distinctive features of ATS drug's molecular structure, notwithstanding new variety of ATS drug, because of its analogous ring substitutes.

This paper aims to propose two variants of more accurate computations, or simply refined, 3D Geometric Moment Invariants (GMI), and compare the performance of proposed refined variants of 3D GMI for ATS drug molecular structure representation. The rest of this paper is organized in this manner. The ensuing section will provide a summary of ATS drug molecular structure similarity search, while Sect. 3 will offer a brief introduction of 3D Geometric Moment Invariants. In Sects. 4 and 5, the proposed more accurate computations of 3D Geometric Moment Invariants techniques are discussed and the experimental setup which describes the dataset preprocessing and experimental design are defined. Furthermore, the results are presented in Sect. 6, and finally, conclusion and future work is formed in Sect. 7.

## 2 ATS drug molecular similarity search

United Nations Office of Drugs and Crime (UNODC) have outlined a set of standard methods to perform identification of ATS drugs to determine the exact, or at least similar, molecular structure. However, forensic laboratories staff occasionally doesn't meticulously follow these standards, hence the fluctuations of results attained from different testing laboratories is expected. However, most of testing laboratories agree that the most effective method for chemical substance identification is Gas Chromatography/Mass Spectrometry (GC/MS) [1–3].

Reference [4] found that GC/MS is imperfect in identifying several varieties of ATS drugs, particularly methamphetamine. There are two stereo-isomers of methamphetamine, which are *l*-methamphetamine and *d*-methamphetamine. Reference [5] terms isomers as “one of several species (or molecular entities) that have the same atomic composition (molecular formula) but different line formulae or different stereo-chemical formulae and hence different physical and/or chemical properties.” Moreover, GC/MS is gradually more powerless in determining numerous substances with altered conformations are actually ATS drugs. Whereas *l*-methamphetamine gives meager pharmacodynamics effect, *d*-methamphetamine in contrast is a controlled substance which is frequently abused and severely addictive [6].

Drugs molecular structure heavily determines the results of manual identification process, which is continuously deteriorated with the introduction of new chemical compositions or conformations. Hence, false positive detection of ATS drugs is regularly occurred due to the flaws of present drug testing unit. Therefore, this study believes that by depending on the global shape of the molecular structure, the identification process can be refined. Molecular structures are often represented by 2D and 3D models. However, the characteristics of the ring substitutes in a molecule are imperceptible in 2D model, as opposed to 3D model. Hence, the latter is vital in discriminating the distinctive features at a ring substitute.

Geometrical shapes have been used for a long time to represent 2D and 3D molecular structures, and these geometric shapes can be describe numerically using shape descriptors. However, there is another type of molecular structure representation in the cheminformatics domain, which is known as molecular descriptors. Molecular descriptors are acquired after molecules are modeled into a molecular representation allowing for mathematical treatment [7]. Many researches are confronted by the difficulties in extracting the image or object shape features which is capable of representing and describing the shape [8].

There are two types of molecular descriptors: topological or 2D descriptors and geometrical or 3D descriptors which derived from a geometrical representation. Since a geometrical representation comprises information of the relative positions of the atoms in 3D space, 3D descriptors generally offer supplementary information and more discrimination rule than 2D descriptors for same molecular structure. There are various 3D molecular descriptors exist, such as 3D-MoRSE descriptors, WHIM descriptors, GETAWAY descriptors, etc.

Invariance with respect to labelling, numbering of the molecule atoms, and molecule translation and rotation is a required property of a molecular descriptor. Furthermore, it also must have an clear algorithmically quantifiable definition, and the values must be

in a appropriate numerical range for the molecule set where it is applicable to [9, 10]. Since a molecular descriptor is independent of the particular characteristics of the molecular representation, it is possible to consider the molecular shape as an image, and thus apply image processing methods to represent the shape of the molecular structure. One of the applications of image processing methods to represent 2D and 3D image is Moment Invariants, which can easily achieve these invariance properties. The first application of Moment Invariants to represent molecular structure is 3D Zernike Descriptors [11].

### 3 3D geometric moment invariants

Moment Invariants (MI) is introduced to describe the objects by a collection of computable magnitudes called invariants using moments that are resistant to certain distortions and that offer sufficient discrimination power to recognize objects belonging to different classes. Moments, on the other hand, are scalar magnitudes employed to characterize an image function and to acquire its distinctive features [12].

MI was first introduced to pattern recognition and image processing by [13], and it is recognized as one of the most vital and regularly engaged 2D and 3D shape descriptors [14]. Although it is subject to numerous fundamental disadvantages, it is often designated as first-choice descriptors and as a benchmark to assess the quality of other shape descriptors [12]. One of the most commonly used moments as a basis of MI construction is Geometric Moments (GM). 3D GM of image intensity function  $f(x, y, z)$  is commonly expressed as [14]:

$$m_{pqr} = \int_{-\infty}^{+\infty} \int_{-\infty}^{+\infty} \int_{-\infty}^{+\infty} x^p y^q z^r f(x, y, z) dx dy dz \quad (1)$$

where  $p, q, r = 0, 1, 2, \dots$ . Conversely, several researches also try to fit the object into a unit box, thus (1) can also be expressed as [15, 16]:

$$m_{pqr} = \int_{-1}^{+1} \int_{-1}^{+1} \int_{-1}^{+1} x^p y^q z^r f(x, y, z) dx dy dz \quad (2)$$

The order of the moment is calculated from the total of  $p, q$ , and  $r$ . A special case of 3D GM is 3D Central Geometric Moments (CGM) [12], which can easily provide translation invariance. It is expressed as:

$$\mu_{pqr} = \int_{-\infty}^{+\infty} \int_{-\infty}^{+\infty} \int_{-\infty}^{+\infty} (x - x_c)^p (y - y_c)^q (z - z_c)^r f(x, y, z) dx dy dz \quad (3)$$

where the center of gravity (centroid) of image intensity function  $f(x, y, z)$  is calculated by  $x_c = \frac{m_{100}}{m_{000}}$ ,  $y_c = \frac{m_{010}}{m_{000}}$ , and  $z_c = \frac{m_{001}}{m_{000}}$ .

Rotation invariance for 3D GM was just recently proposed by [17] using moment tensor method. The authors proposed 1185 invariants constructed from moments of order 2 until order 16. The first 2 rotation invariants are presented as follows:

$$I_1 = (\mu_{200} + \mu_{020} + \mu_{002})/\mu_{000}^2 \tag{4}$$

$$I_2 = (\mu_{200}^2 + \mu_{020}^2 + \mu_{002}^2 + 2\mu_{110}^2 + 2\mu_{101}^2 + 2\mu_{011}^2)/\mu_{000}^4 \tag{5}$$

The zeroth-order moment ( $m_{000}$ ) is used as divisor to normalize the GM with respect to scaling. Therefore, 3D Geometric Moment Invariants (3D GMI) is the term coined to express 3D GM which is invariance with respect to translation, scale, and rotation transformations.

#### 4 Refined 3D geometric moment invariants

A digital 3D image of size  $N \times N \times N$  is an array of voxels (volume pixels), therefore the triple integral in (1) is substituted by triple summation. The most frequently used procedure is to employ the rectangular, i.e., zero-order method of numeric integration. And thus, (1) takes the following discrete form:

$$\hat{m}_{pqr} = \sum_{i=1}^N \sum_{j=1}^N \sum_{k=1}^N i^p j^q k^r f_{ijk} \tag{6}$$

where  $i, j, k$  are coordinates of the voxels and  $f_{ijk}$  is the gray-level of the voxel  $i, j, k$ . It should be noted that  $\hat{m}_{pqr}$  is just an approximation of  $m_{pqr}$ .

However, [18] and later generalized by [19], proposes a formula to obtain a more precise estimation for calculating 2D GM, where the author integrate the monomials  $x^p y^q$  precisely by the Newton–Leibnitz formula on each pixel, which is so-called Precise Geometric Moments (PGM):

$$\begin{aligned} \dot{m}_{pq} &= \sum_{i=1}^N \sum_{j=1}^N f_{ij} \int \int_{A_{ij}} x^p y^q dx dy \\ &= \frac{1}{(p+1)(q+1)} \sum_{i=1}^N \sum_{j=1}^N U_p(i)U_q(j) f_{ij} \end{aligned} \tag{7}$$

$$U_s(a) = (a + 0.5)^{s+1} - (a - 0.5)^{s+1} \tag{8}$$

This study proposes the extension of 2D PGM into 3D PGM and thus (7) takes the following form:

$$\begin{aligned} \dot{m}_{pqr} &= \sum_{i=1}^N \sum_{j=1}^N \sum_{k=1}^N f_{ijk} \int \int \int_{A_{ijk}} x^p y^q z^r dx dy dz \\ &= \frac{1}{(p+1)(q+1)(r+1)} \sum_{i=1}^N \sum_{j=1}^N \sum_{k=1}^N U_p(i)U_q(j)U_r(k) f_{ijk} \end{aligned} \tag{9}$$

where  $A_{ij}$  and  $A_{ijk}$  denotes the area of the pixel  $(i, j)$  and voxel  $(i, j, k)$  respectively. Equations (7) and (9) are still a zero-order approximation of moments of the original image, but only the image is approximated, the monomials are integrated precisely.

On the other hand, centers of these aforementioned voxels are the points  $(x_i, y_j, z_k)$ , where the image intensity function is defined only for this discrete set of points  $(x_i, y_j, z_k) \in [-1, 1] \times [-1, 1] \times [-1, 1]$ .  $\Delta x_i = x_{i+1} - x_i$ ,  $\Delta y_j = y_{j+1} - y_j$ , and  $\Delta z_k = z_{k+1} - z_k$  are sampling intervals in the  $x$ -,  $y$ -, and  $z$ -directions, respectively. In the literature of digital image processing, the intervals  $\Delta x_i$ ,  $\Delta y_j$ , and  $\Delta z_k$  are fixed at constant values  $\Delta x_i = \Delta x = 2/N$ ;  $\forall i$ ,  $\Delta y_j = \Delta y = 2/N$ ;  $\forall j$ ,  $\Delta z_k = \Delta z = 2/N$ ;  $\forall k$ . Therefore, the set of points  $(x_i, y_j, z_k)$  will be expressed as follows:

$$n_a = -1 + (a - 0.5) \Delta n \tag{10}$$

with  $a = 1, 2, 3, \dots, N$ . For the discrete-space version of the image, (2) is usually approximated as:

$$\hat{m}_{pqr} = \sum_{i=1}^N \sum_{j=1}^N \sum_{k=1}^N x_i^p y_j^q z_k^r f(x_i, y_j, z_k) \Delta x \Delta y \Delta z \tag{11}$$

Equation (11) is purported as direct method for GM computation, which is the approximated version using zero-order approximation. As indicated by [20], (11) is not a very accurate approximation of (2). The author proposed to use the approximated form to improve the accuracy, which is then refined by [16]. The formula is then extended into 3D form, which has been presented in the previous publication of this study [21]:

$$\ddot{m}_{pqr} = \sum_{i=1}^N \sum_{j=1}^N \sum_{k=1}^N V_p(i) V_q(j) V_r(k) f(x_i, y_j, z_k) \tag{12}$$

$$U_s(a) = \int_{n_a - \frac{\Delta n}{2}}^{n_a + \frac{\Delta n}{2}} n^s dn = \frac{1}{s + 1} \left[ I_{a+1}^{s+1} - I_a^{s+1} \right] \tag{13}$$

$$I_{a+1} = n_a + \frac{\Delta n}{2} = -1 + a \Delta n; I_a = n_a - \frac{\Delta n}{2} = -1 + (a - 1) \Delta n \tag{14}$$

The basis of the formula is alternative extended Simpson's rule, proposed by [20]. The rule was used to evaluate the triple integral defined by (2), and calculate exactly the GM, thus it is known as Exact Geometric Moments (EGM). However, it is rather difficult to achieve translation invariance by calculating accurately CGM, either by using (9) or (12). Fortunately, [22] provides a relationship between central and non-central moments for regular GM, and defines a convenient formula to calculate central moments from non-central moments, and vice versa:

$$\mu_{pqr} = \sum_{a=0}^p \sum_{b=0}^q \sum_{c=0}^r \binom{p}{a} \binom{q}{b} \binom{r}{c} m_{100}^{p-a} m_{010}^{q-b} m_{001}^{r-c} (-m_{000})^{-(p+q+r-a-b-c)} m_{abc} \tag{15}$$



$$m_{pqr} = \sum_{a=0}^p \sum_{b=0}^q \sum_{c=0}^r \binom{p}{a} \binom{q}{b} \binom{r}{c} m_{100}^{p-a} m_{010}^{q-b} m_{001}^{r-c} m_{000}^{-(p+q+r-a-b-c)} \mu_{abc} \quad (16)$$

Despite the fact (15) and (16) were intended for regular GM, this study found that (15) can also be used to compute Central Precise Geometric Moments [23] and Central Exact Geometric Moments [21]. These central moments are then used to derive 3D rotation invariants by using moment tensor method, thus the proposed techniques are known as 3D Precise Geometric Moment Invariants (3D PGMI) and 3D Exact Geometric Moment Invariants (3D EGMI) [21], respectively. In the next section, the performance of both techniques on ATS and non-ATS dataset is revealed.

## 5 Experimental setup

Through the objectives specified in the previous section, a pragmatic comparative study is planned and performed. This section delivers a comprehensive report of the experimental setup.

### 5.1 Dataset preprocessing

The process of converting 2D molecular structure into proposed 3D molecular structure representations is described in this section. Images of ATS drug 2D molecular structure employed in this study are collected from [24], which enlist a total of 3595 potentially and typically abused ATS drugs. Subsequently, 3595 images of non-ATS (n-ATS) drug 2D molecular structure are also randomly acquired from [25]. Both 2D molecular structure image sets are gathered and yield a total number of 7190 images of 2D molecular structures for training and testing sets.

First of all, MarvinSketch 15.11.9 [26] will be used to redraw all 2D molecular structure images in a standard notation, clean the structures, and lastly transform the structures into 3D molecular structure. These 3D molecular structures are stored as MDL MOL file. An example of 2D and 3D molecular structure of ATS and n-ATS drugs is shown in Figs. 1 and 2, respectively. The proposed techniques require 3D array of voxels for its input. A software called binvox 1.21 [27] can be used to produce 3D array of voxels, however it requires 3D Virtual Reality Markup Language (VRML) object as its input. Fortunately, a software called Jmol 14.4.0 [28] is capable of converting MDL MOL file to VRML file.

As mentioned earlier, VRML file is voxelated as 3D array of voxels with size of  $512 \times 512 \times 512$  grid for the training set, and it is uniquely and randomly translated and rotated 90 degrees incrementally in  $x$ -,  $y$ -, and  $z$ -axis as the testing set. After the 3D arrays of voxels have been produced, the invariants for training and testing set will be computed from moments of order 0 until order 16 using 3D PGMI and 3D EGMI. An example of the voxelated 3D molecular structure is depicted in Fig. 3 and the invariants computed from the proposed techniques are presented in Table 1, respectively.

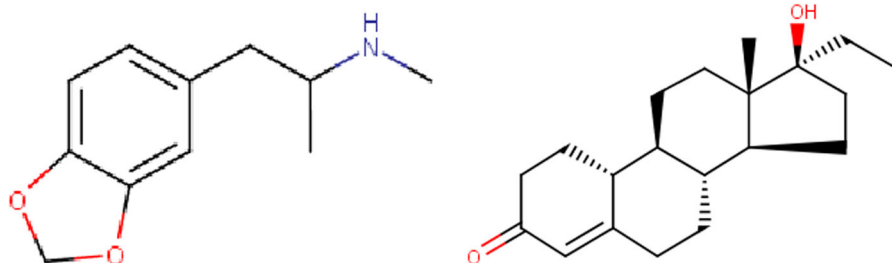


**Fig. 1** 2D molecular structure of ATS drug, ecstasy (*left*) and n-ATS drug, norethandrolone (*right*), drawn using MarvinSketch [26]

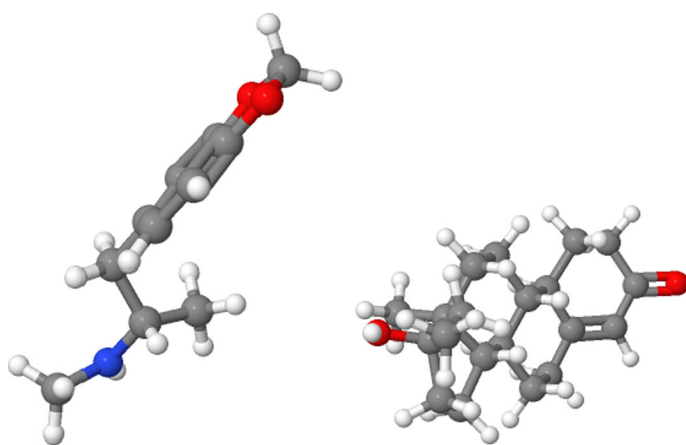


**Fig. 2** 3D molecular structure of ATS drug, ecstasy (*left*) and n-ATS drug, norethandrolone (*right*), converted using Jmol [28]

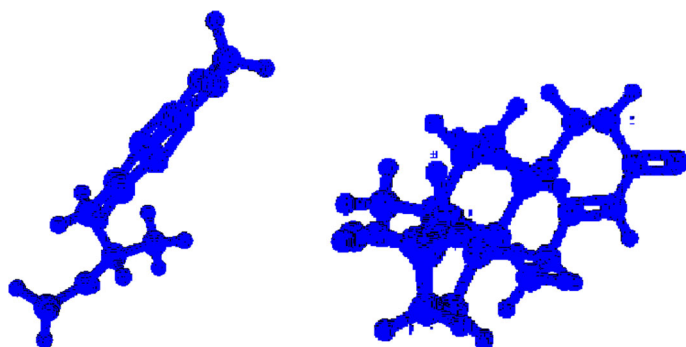


**Fig. 3** 3D molecular structure of ATS drug, ecstasy (*left*) and n-ATS drug, norethandrolone (*right*), voxelated using binvox [27]

**Table 1** Invariants of the proposed MI techniques

Structure name	MI	F1	F2	...	F1184	F1185
Ecstasy	3D PGMI	2.139E10	1.784E10	...	3.762E24	6.057E43
	3D EGMI	0.019456	0.016225	...	0.012157	0.010609
Norethandrolone	3D PGMI	2.792E10	2.233E10	...	5.788E24	1.300E44
	3D EGMI	0.025398	0.020310	...	0.018703	0.022781

## 5.2 Experimental design

This paper employs customary structure of pattern recognition, which consists of preprocessing, feature extraction, and classification phase, and compares the performance of the proposed 3D PGMI and 3D EGMI. It is also worth mentioning that there are actually two types of moments to be used compute invariants, and two types of magnitude normalization of the invariants [17]. The first type of moments is volume moments, which compute the moments from all voxels, and the second type is surface moments, which only compute moments by double integration over the outer-most voxels. On the other hand, the two types of magnitude normalization are normalization with respect to degree and with respect to weight. Both MIs in this study are computed as volume moments and normalized to its respective degree.

All computed invariants are evaluated for its processing time, memory consumption, and classification accuracy, which are executed for 23 times. This is because, although there are 64 possible orientations if an image is rotated 90 degrees incrementally in  $x$ -,  $y$ -, and  $z$ -axis, there are actually only 24 distinct orientation exist. Hence, non-rotated version of the drug molecular structure will be used as training set; while the remaining 23 rotated versions will be used as the testing set. An example of the rotated versions of an ATS drug is illustrated in Fig. 4. As a final point, the invariants computed by both proposed techniques are evaluated against renowned classifier, Random Forest [29], and using Leave-One-Out strategy.

## 6 Experimental results and discussion

The proposed techniques will be evaluated numerically by computing invariant 1 to 1185 for all 7190 molecular structures in this section. The investigations are aimed to evaluate the merit and the consistency of both proposed MI techniques.

### 6.1 Processing time and memory consumption

The frequently used benchmarks for evaluating the merit of machine learning algorithms are classification accuracy and processing time. However, this study also considers an additional benchmark, which is memory consumption. This examination will compare the merit of the proposed techniques in order to determine the most

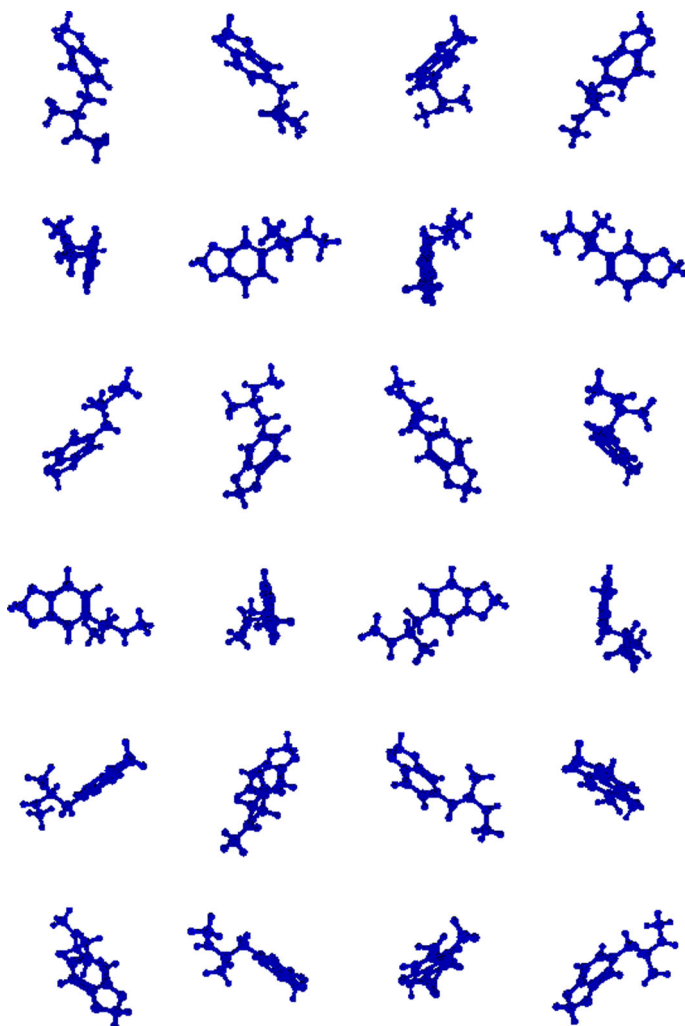


**Fig. 4** Rotated versions of ecstasy 3D molecular structure

suitable MI method to represent molecular structure. Figures 5 and 6 present the mean of processing time and memory consumption for each MIs respectively.

## 6.2 Classification of unfamiliar ATS drug molecular structure

Comparing the classification accuracy of 3D PGMI and 3D EGMI is also one of the primary objectives of this paper. Table 2 presents the mean classification accuracy results from 23 testing set using Random Forest classifier.

As presented in Table 2, it is obvious that 3D PGMI yields slightly higher results of mean processing time, memory usage, and classification accuracy. However, to

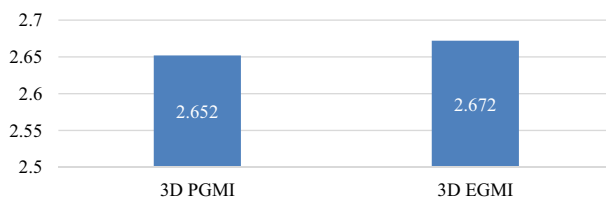


**Fig. 5** Mean processing time for proposed MI techniques (in s)

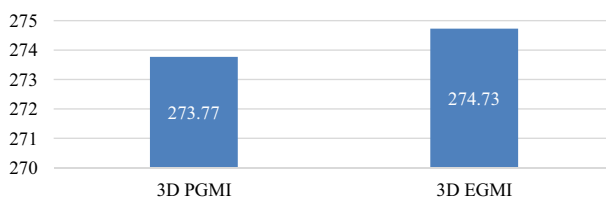


**Fig. 6** Mean memory consumption for proposed MI techniques (in MB)

**Table 2** Mean classification accuracy for proposed MI techniques

MI	Mean accuracy (%)
3D PGMI	73.90
3D EGMI	73.20

further corroborate the merit of 3D PGMI as opposed to 3D EGMI, thorough statistical validation using independent samples *t*-test must be performed using SPSS 17 software. There was a statistically significant difference in the accuracy using 3D EGMI ( $\mu = 0.7320$ ,  $\sigma = 0.0008$ ) and 3D PGMI ( $\mu = 0.7390$ ,  $\sigma = 0.0010$ );  $t(44) = 26.5022$ ,  $p = 0.000$ . This result suggests that the 3D PGMI is capable to differentiate the distinctive features of ATS drugs and n-ATS drugs at a ring substitute. Although it is evident that 3D EGM is inferior to 3D PGM, it still can be applied as a basis to indirectly compute orthogonal (OG) moments, especially continuous OG moments on a cube or sphere, such as Legendre and Zernike moments. On the other hand, 3D PGM can also be applied as a basis to indirectly compute discrete OG moments on a cube, most notably Discrete Chebyshev and Hahn moments.

## 7 Conclusion and future works

Two refined 3D Geometric Moment Invariants have been proposed to represent drug molecular structure, and an exhaustive comparative study on the proposed MI techniques has been presented. This paper compared the merits of 3D Precise Geometric Moment Invariants (3D PGMI) and 3D Exact Geometric Moment Invariants (3D EGMI). Although the evaluations have shown that 3D PGMI produces the slightly higher results as opposed to 3D EGMI, this study nonetheless functions as a stepping stone towards better molecular structure representation, especially for computing continuous and discrete orthogonal moments from 3D EGM and 3D PGM.

Hence, future works to integrate 3D EGM and 3D PGM into OG moments, which is expected to provide better representation of molecular structure, is required. The proposed molecular representation techniques will also be evaluated using customized classifiers for shape representation, and compared against existing and well-known 3D molecular descriptors.

**Acknowledgements** This study is supported by UTeM Postgraduate Fellowship (Zamalah) Scheme from Universiti Teknikal Malaysia Melaka (UTeM), Malaysia and Collaborative Research Programme (CRP)—ICGEB Research Grant (CRP/MYS13-03) from International Centre for Genetic Engineering and Biotechnology (ICGEB), Italy.

## References

1. L.J. Langman, L.D. Bowers, J.A. Collins, C.A. Hammett-Stabler, M.A. LeBeau, *Gas Chromatography/mass Spectrometry Confirmation of Drugs; Approved Guidelines*, 2nd edn. (Clinical and Laboratory Standards Institute, Pennsylvania, 2010)
2. United Nations Office of Drugs and Crime: Recommended Methods for the Identification and Analysis of Amphetamine, Methamphetamine and Their Ring-substituted Analogues in Seized Materials, in vol. Sales No. E.06.XI.1. UNODC, New York (2006)
3. D.-L. Lin, R.-M. Yin, L.H. Ray, Gas chromatography–mass spectrometry (GC–MS) analysis of amphetamine, methamphetamine, 3,4-methylenedioxymphetamine and 3,4-methylenedioxymethamphetamine in human hair and hair sections. *J. Food Drug Anal.* **13**(3), 193–200 (2005)
4. J.J. McShane, GC-MS is Not Perfect: The Case Study of Methamphetamine (2011). <http://www.theuthaboutforensicscience.com/gc-ms-is-not-perfect-the-case-study-of-methamphetamine/>. Accessed 26 Nov 2012
5. International Union of Pure and Applied Chemistry: Compendium of Chemical Terminology, 2nd edn. Gold Book. (Blackwell Scientific Publications, Oxford, 2006)
6. J. Mendelson, N. Uemura, D. Harris, R.P. Nath, E. Fernandez, P. Jacob III, E.T. Everhart, R.T. Jones, Human pharmacology of the methamphetamine stereoisomers. *Clin. Pharmacol. Ther.* **80**(4), 403–420 (2006). doi:10.1016/j.clpt.2006.06.013
7. R. Todeschini, V. Consonni, Descriptors from molecular geometry, in *Handbook of Chemoinformatics*. (Wiley-VCH Verlag GmbH, 2008), pp. 1004–1033
8. A.K. Muda, *Authorship Invarianceness for Writer Identification Using Invariant Discretization and Modified Immune Classifier*. Universiti Teknologi Malaysia (2009)
9. V. Consonni, R. Todeschini, Basic Requirements for Valid Molecular Descriptors (2006). [http://www.moleculardescriptors.eu/tutorials/T3\\_moleculardescriptors\\_requirements.pdf](http://www.moleculardescriptors.eu/tutorials/T3_moleculardescriptors_requirements.pdf)
10. M. Randić, Molecular bonding profiles. *J. Math. Chem.* **19**(3), 375–392 (1996). doi:10.1007/bf01166727
11. D. Kihara, L. Sael, R. Chikhi, J. Esquivel-Rodriguez, Molecular surface representation using 3D Zernike descriptors for protein shape comparison and docking. *Curr. Protein Pept. Sci.* **12**, 520–530 (2011)
12. J. Flusser, T. Suk, B. Zitová, *Moments and Moment Invariants in Pattern Recognition*, vol. 1 (Wiley, West Sussex, 2009)
13. M.-K. Hu, Visual pattern recognition by moment invariants. *IRE Trans. Inf. Theory* **8**(2), 179–187 (1962). doi:10.1109/TIT.1962.1057692
14. F.A. Sadjadi, E.L. Hall, Three-dimensional moment invariants. *IEEE Trans. Pattern Anal. Mach. Intell.* **2**(2), 127–136 (1980). doi:10.1109/TPAMI.1980.4766990
15. K.M. Hosny, Exact and fast computation of geometric moments for gray level images. *Appl. Math. Comput.* **189**(2), 1214–1222 (2007). doi:10.1016/j.amc.2006.12.025
16. P.T. Yap, R. Paramesran, An efficient method for the computation of Legendre moments. *IEEE Trans. Pattern Anal. Mach. Intell.* **27**(12), 1996–2002 (2005). doi:10.1109/TPAMI.2005.232
17. T. Suk, J. Flusser, Tensor method for constructing 3D moment invariants, in *Computer Analysis of Images and Patterns, Sevilla, Spain 2011*, ed. by A. Berciano, D. Díaz-Pernil, W.G. Kropatsch, H. Molina-Abril, P. Real (Springer, Berlin, 2011), pp. 213–219

18. W.-G. Lin, S.-S. Wang, A note on the calculation of moments. *Pattern Recognit. Lett.* **15**(11), 1065–1070 (1994). doi:[10.1016/0167-8655\(94\)90121-x](https://doi.org/10.1016/0167-8655(94)90121-x)
19. J. Flusser, Refined moment calculation using image block representation. *IEEE Trans. Image Process.* **9**(11), 1977–1978 (2000). doi:[10.1109/83.877219](https://doi.org/10.1109/83.877219)
20. S.X. Liao, M. Pawlak, On image analysis by moments. *IEEE Trans. Pattern Anal. Mach. Intell.* **18**(3), 254–266 (1996). doi:[10.1109/34.485554](https://doi.org/10.1109/34.485554)
21. S.F. Pratama, A.K. Muda, Y.-H. Choo, A. Abraham, Exact computation of 3D geometric moment invariants for ATS drugs identification, in *Innovations in Bio-Inspired Computing and Applications, vol. 424. Advances in Intelligent Systems and Computing*, ed. by V. Snášel, A. Abraham, P. Krömer, M. Pant, A.K. Muda (Springer, Berlin, 2016), pp. 347–358
22. D. Xu, H. Li, Geometric moment invariants. *Pattern Recognit.* **41**(1), 240–249 (2008)
23. S.F. Pratama, A.K. Muda, Y.-H. Choo, A. Abraham, 3D geometric moment invariants for ATS drugs identification: a more precise approximation, in *Proceedings of the 16th International Conference on Hybrid Intelligent Systems (HIS 2016)*, ed. by A. Abraham, A. Haqiq, A.M. Alimi, G. Mezzour, N. Rokbani, A.K. Muda (Springer, Cham 2017) pp. 124–133 (2017)
24. Isomer Design: [pikhal.info](http://pikhal.info) (2015)
25. Royal Society of Chemistry: ChemSpider Database (2015)
26. ChemAxon Ltd.: Marvin (2016). <http://www.chemaxon.com>
27. Min, P.: binvox 3D mesh voxelizer (2016). <http://www.patrickmin/binvox>
28. Jmol: Jmol: an open-source Java viewer for chemical structures in 3D (2016). <http://www.jmol.org/>
29. L. Breiman, Random Forests. *Machine Learning*, **45**(1), 5–32 (2001). doi:[10.1023/A:1010933404324](https://doi.org/10.1023/A:1010933404324)